Int. J. Heat Mass Transfer. Vol. 37, No. 2, pp. 185–194, 1994
Printed in Great Britain

0017–9310/94 $6.00+0.00

Heat transfer to mixtures of acetone, isopropanol and water under subcooled flow boiling conditions—II. Prediction of heat transfer coefficients

U. WENZEL
Department of Chemical and Materials Engineering, University of Auckland, Auckland, New Zealand

and

H. MÜLLER-STEINHAGEN†
Department of Chemical and Process Engineering, University of Surrey, Guildford GU2 5XH, U.K.

(*Received* 24 *July* 1992 *and in final form* 27 *August* 1993)

Abstract—A model is presented, which predicts local heat transfer coefficients under subcooled flow boiling conditions for mixtures, covering the regimes of convective heat transfer, transition region and fully developed nucleate boiling. While the present model is valid for annular flow, it can be easily adopted to tubular flow conditions. The predictions of this model are compared with experimental data for binary and ternary mixtures.

INTRODUCTION

A CONSIDERABLE amount of research has gone into the development of models predicting convective and pool boiling heat transfer coefficients. Several publications [1, 2] have shown that the superposition of convective and pool boiling heat transfer can be used to predict flow boiling heat transfer coefficients. This method was, for instance, suggested by Chen in ref. [3]. However, to-date the use of existing models is restricted either to single component fluids or to fully developed nucleate boiling heat transfer. The calculation procedure presented in this paper is not limited by those restrictions. It predicts heat transfer from the convective regime up to the fully developed boiling regime for single component fluids and for polynary mixtures under saturated and sub-cooled flow boiling conditions. The model has been verified against all data presented in Part I of this paper. All correlations used in this model have been left in their original form, i.e. none of the parameters were adjusted to fit the available set of data.

DESCRIPTION OF MODEL

The model is based on an additive superposition of convective and boiling heat transfer coefficients

$$\dot{q} = \alpha_{\text{conv,tp}} \cdot (T_w - T_b) + \alpha_{\text{boil}} \cdot S \cdot (T_W - T_{\text{Sat}}) \quad (1)$$

where

$$\alpha_{\text{conv,tp}} = f(\alpha_{\text{conv}}, F). \quad (2)$$

† Author to whom correspondence should be addressed.

The enhancement factor F takes into account the increased heat transfer due to the co-current flow of liquid and vapour. The suppression of nucleate boiling, which is caused by the steepening of the temperature gradient in the liquid film due to forced convection is considered by the suppression factor S. This factor is defined as: '. . . the ratio of the mean superheat seen by the growing bubble to the wall superheat . . .', (Collier [4]). The factors F and S were first introduced by Chen in ref. [3]. The boiling heat transfer coefficient is only calculated for wall temperatures higher than the saturation temperature of the liquid.

Figure 1 shows a flow diagram of the model, illustrating the calculation procedure. The major calculation steps are explained below, in order of their appearance in the flow diagram.

Input data

Input data are heat flux, fluid composition, temperature, velocity and pressure. The calculation can be easily modified if the wall temperature is known rather than the heat flux.

Enhancement factor F and suppression factor S

Based on experimental data, Collier presents the following empirical correlations for F and S [4]:

$$F = 1 \quad \text{for} \quad \frac{1}{X_{tt}} \leqslant 0.1$$

$$F = 2.35\left(\frac{1}{X_{tt}} + 0.213\right)^{0.736} \quad \text{for} \quad \frac{1}{X_{tt}} \geqslant 0.1 \quad (3)$$

NOMENCLATURE

Bo	boiling number [—]
c_p	specific heat [kJ kg^{-1} K^{-1}]
d	diameter [m]
f	friction factor [—]
f_i	Fanning friction factor [—]
F	enhancement factor [—]
F_p	pressure function [—]
Gr	Grashof number [—]
h	enthalpy [kJ kg^{-1}]
Δh_v	latent heat of evaporation [kJ kg^{-1}]
l_{th}	heated length to thermocouple location [m]
$\dot{m}$	mass flux [kg m^{-2} s^{-1}]
M	molar weight [kg kmol^{-1}]
n	exponent [—]
$\dot{n}$	total molar flux [kmol m^{-2} s^{-1}]
Nu	Nusselt number [—]
p^*	reduced pressure, p/p_c [—]
Pe	Peclet number [—]
Ph	phase change number [—]
Pr	Prandtl number [—]
$\dot{q}$	heat flux [W m^{-2}]
r	radius [m]
$\dot{r}$	relative evaporation rate [—]
r^*	radius ratio for annulus [—]
r_m^*	radius ratio of zero shear stress [—]
R_p	surface roughness [μm]
Re	Reynolds number [—]
s	film thickness [m]
S	suppression factor
T	temperature [K]
x	mole fraction in liquid [—]
X_{tt}	Martinelli parameter [—]
y	mole fraction in vapour [—].

Greek symbols

α	heat transfer coefficient [W m^{-2} K^{-1}]
β	mass transfer coefficient [m s^{-1}]
δ	diffusion coefficient [m^2 s^{-1}]
λ	thermal conductivity [W m^{-1} K^{-1}]
μ	dynamic viscosity [kg m^{-1} s^{-1}]
ρ	molar density [kmol m^{-3}].

Indices

b	bulk
boil	boiling
conv	convective
dev	developing
f	fluid
g	gas
h	hydraulic
i	inner
id	ideal
l	liquid
lam	laminar
o	outer
Ph	interface
Sat	saturation
tp	two phase
turb	turbulent
W	wall
∞	fully developed.

$$S = \frac{1}{1+2.53\times10^{-6}Re_{tp}^{1.17}} \tag{4}$$

with:

$$Re_{tp} = \frac{\dot{m}(1-x)d_h}{\mu_l}\cdot F^{1.25}. \tag{5}$$

The parameter X_{tt} in equation (3) is the so called Martinelli Parameter, which is a function of the vapour mass fraction:

$$X_{tt} = \left(\frac{1-x}{x}\right)^{0.9}\left(\frac{\rho_g}{\rho_l}\right)^{0.5}\left(\frac{\mu_l}{\mu_g}\right)^{0.1} \tag{6}$$

where the vapour mass fraction x is defined as:

$$x = \frac{\dot{m}_g}{\dot{m}_g+\dot{m}_l}. \tag{7}$$

To calculate the enhancement and suppression factors, the local vapour mass fraction has to be determined. Schröder presents a calculation method in ref. [5] for the local vapour mass fraction, which is applicable for subcooled and saturated boiling. To illustrate this method, Fig. 2 shows the different heat transfer regimes encountered by a subcooled liquid entering a heated tube. The mean fluid temperature and the vapour mass quality are plotted over the length of the tube. Between the inlet of the tube and line A heat is transferred to the fluid by single phase convection. At line A the first vapour bubbles are created and the subcooled boiling region begins. The bubbles collapse either at the wall or close to it, because the mean fluid temperature is still considerably lower than the saturation temperature. This occurs up to line B in the diagram, where the mean fluid temperature is high enough to permit the existence of vapour bubbles in the bulk of the liquid. The vapour mass fraction, which was zero up to this point, starts to increase. The mean temperature of the fluid, which now consists of liquid and vapour, reaches the saturation temperature at line C in the diagram. This is the onset of the bulk boiling regime. Schröder [5] uses a correlation by Levy [6] to calculate the local vapour mass fraction:

$$x = Ph - Ph_n\exp\left(\frac{Ph}{Ph_n}-1\right) \tag{8}$$

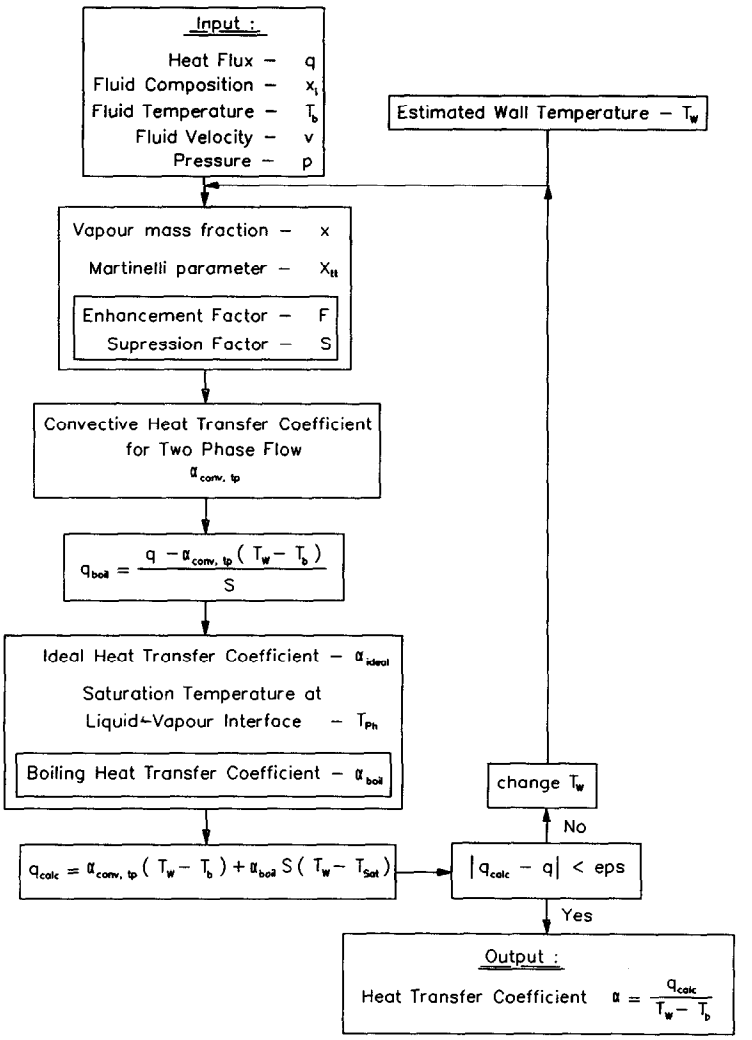

FIG. 1. Flow diagram of model.

where Ph is the so called phase change number and is defined as:

$$Ph = \frac{\bar{h}_f - h_{l,Sat}}{\Delta h_v}. \tag{9}$$

This number describes the local thermodynamic condition of the fluid. As long as the mean fluid stream is subcooled, Ph has negative values. Ph becomes positive and equivalent to the local vapour mass fraction, if the mean enthalpy of the fluid is higher than the saturation enthalpy of the liquid. Ph_n is the value of the phase change number which is reached, once the mean fluid temperature is high enough to permit the existence of vapour bubbles in the bulk of the liquid. The location where this is taking place, is indicated by line B in Fig. 2. Schröder [5] suggests to calculate Ph_n with a correlation valid for laminar and turbulent flow using the boiling number Bo and the Peclet number Pe:

$$Ph_n = \frac{-Bo}{\left[\left(\frac{455}{Pe}\right)^2 + 0.0065^2\right]^{1/2}} \tag{10}$$

with:

$$Bo = \frac{\dot{q}}{\dot{m}\Delta h_v} \quad \text{and} \quad Pe = \frac{\dot{m} c_p d_h}{\lambda}.$$

The local vapour mass fraction is estimated using equations (8)–(10). The Martinelli Parameter is then calculated with equation (6). The enhancement and suppression factors are evaluated with correlations (3) and (4).

Convective heat transfer coefficient for two phase flow

Chen [3] used the Dittus/Boelter correlation [7] for turbulent flow to calculate the convective heat transfer coefficient to the liquid

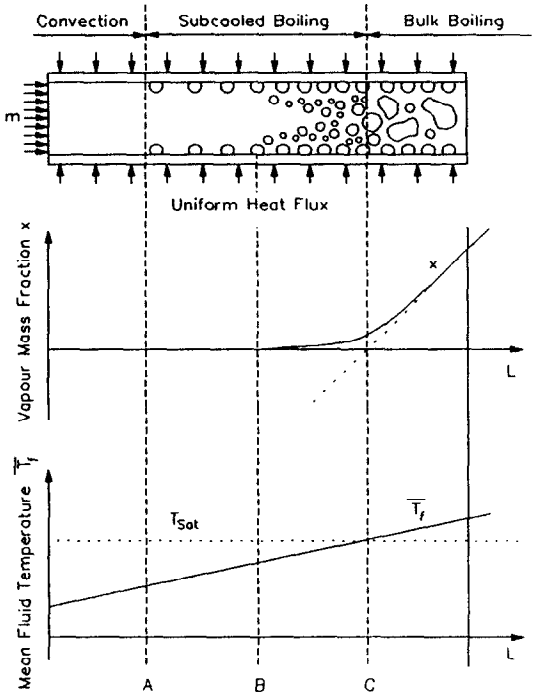

FIG. 2. Local vapour mass fraction and mean fluid temperature in subcooled boiling.

$$\alpha_l = \frac{\lambda_l}{d_h} \cdot Re_l^{0.8} \cdot Pr_l^{0.4}. \tag{11}$$

To take into account the two phase flow situation, the Reynolds number of the liquid is multiplied with the enhancement factor F to the power of 1.25:

$$\alpha_{tp} = \frac{\lambda_l}{d_h} \cdot (Re_l \cdot F^{1.25})^{0.8} \cdot Pr_l^{0.4} \tag{12}$$

which is in this case equivalent to a multiplication of the heat transfer coefficient of the liquid by F. In this paper a different approach is used, since more reliable correlations for convective heat transfer have become available. A superposition of the laminar and turbulent heat transfer coefficients is used for Reynolds numbers below 10 000; for higher Reynolds numbers only the turbulent heat transfer coefficient is considered:

$$\alpha_{conv.tp} = \sqrt[3]{(\alpha_{lam}^3 + \alpha_{turb}^3)} \quad \text{for} \quad Re \leqslant 10\,000$$
$$\alpha_{conv.tp} = \alpha_{turb} \quad \text{for} \quad Re \geqslant 10\,000. \tag{13}$$

Variations in the physical properties of the fluid due to the wall superheat are accounted for by multiplying the heat transfer coefficient with the viscosity ratio at bulk and wall temperature to the power of 0.11, as suggested by Gnielinski in ref. [8].

The *laminar heat transfer coefficient* in equation (13) is calculated by a superposition of the Nusselt numbers for fully developed and for developing flow using a recommendation of Schlünder in ref. [9]

$$\alpha_{lam} = \frac{\lambda}{d_h} \cdot \sqrt[3]{(Nu_\infty^3 + Nu_{dev}^3)}. \tag{14}$$

All data used for comparison with the model were measured in a concentric annular test-section. A constant heat flux was applied to the inside wall while the outside wall was insulated. Shah and London [10] define this situation as a fundamental boundary condition of the second kind and give the fully developed Nusselt number in this case as:

$$Nu_\infty = 6.487912. \tag{15}$$

Because of the particular geometry of the test section (see Part I of this paper) the flow inside the annulus is hydrodynamically fully developed and thermally developing. The Nusselt number for thermally developing flow inside an annulus with boundary conditions of the second kind is given by Shah and London [10]:

$$Nu_{dev} = 0.517(f_i Re)^{1/3}\left(\frac{Pe\, d_h}{l_{th}}\right)^{1/3}. \tag{16}$$

Lundberg *et al.* [11, 12] give the Fanning friction factor f_i for laminar flow on the inside wall of an annulus as:

$$f_i = \frac{16(1-r^*)}{1+r^{*2}-2r_m^{*2}} \cdot \frac{r_m^{*2}-r^{*2}}{r^* Re} \tag{17}$$

with:

$$r^* = \frac{r_i}{r_o} \quad \text{and} \quad r_m^* = \left(\frac{1-r^{*2}}{2\ln(1/r^*)}\right)^{1/2}.$$

To calculate the *turbulent heat transfer coefficient* in equation (13) a correlation by Petukhov and Popov [13] is used. It is multiplied with a factor by Hausen [14] to give the local heat transfer coefficient for thermally developing flow and with a factor by Petukhov and Roizen [15] to take annular flow into account:

$$\alpha_{turb} = \frac{\lambda}{d_h} \cdot \frac{f/8 RePr}{1+12.7\sqrt{(f/8)}(Pr^{2/3}-1)} \cdot \left(1+\frac{1}{3}\left(\frac{d_h}{l_{th}}\right)^{2/3}\right) \cdot 0.86\left(\frac{d_i}{d_o}\right)^{-0.16}. \tag{18}$$

The friction factor f is given by Filonenko in ref. [16]:

$$f = (1.82 \cdot \log Re - 1.64)^{-2}. \tag{19}$$

The Reynolds number used in equations (16), (18), (19) is the two phase Reynolds number

$$Re_{tp} = \frac{(1-x)\dot{m} d_h}{\mu} \cdot F^{1.25}. \tag{20}$$

For vertical upward flow, the effect of natural convection may be considered by a superposition, which is suggested by Schlünder in ref. [17]

$$Re = \sqrt{(Re_{tp}^2 + Gr/2.5)}. \tag{21}$$

However, in almost all practical applications $Re_{tp}^2 \gg Gr$.

Nucleate boiling heat transfer coefficient

The calculation of the nucleate boiling heat transfer coefficient is only initiated if the wall temperature is higher than the saturation temperature. For lower wall temperatures the boiling heat transfer coefficient is set to zero.

The heat transfer under boiling conditions is a function of heat flux and fluid composition. Gropp and Schlünder show in ref. [18] that the reduction of the heat transfer coefficient observed for liquid mixtures is caused by the liquid-side mass transfer resistance. Because of the preferential evaporation of the more volatile component, the mass transfer resistance results in a higher saturation temperature at the vapour/liquid interface. This saturation temperature is used by Schlünder [18] to correlate the heat transfer coefficient of mixtures

$$\alpha_{boil} = \frac{\alpha_{id}}{1+(\alpha_{id}/\dot{q}_{boil})(T_{Ph}-T_{Sat})}. \tag{22}$$

The ideal heat transfer coefficient α_{id} in equation (22) represents the heat transfer to a single-component liquid, which has the same physical properties as the mixture. It can be estimated from the heat transfer coefficients of various components of the mixture

$$\alpha_{id} = \left(\sum_{i=1}^{n} \frac{x_i}{\alpha_i}\right)^{-1}. \tag{23}$$

There are various correlations to predict heat transfer coefficients for flow boiling of pure liquids. Several researchers [1, 2] recommend to use correlations developed for pool boiling conditions even though forced convection is present. One of the most reliable pool boiling correlations was developed by Gorenflo [19]

$$\frac{\alpha}{\alpha_o} = F_p\left(\frac{\dot{q}}{\dot{q}_o}\right)^n\left(\frac{R_p}{R_{po}}\right)^{0.113}. \tag{24}$$

The pressure function F_p and the exponent n are calculated using the reduced pressure p^*:

for organic liquids

$$F_p = 2.1\cdot p^{*0.27} + \left(4.4+\frac{1.8}{1-p^*}\right)\cdot p^* \tag{25}$$

for water and low boiling liquids

$$F_p = 2.55\cdot p^{*0.27} + \left(9+\frac{1}{1-p^{*2}}\right)\cdot p^{*2}. \tag{26}$$

The exponent n is calculated from

$$n = 0.9-0.3\cdot p^{*a} \tag{27}$$

with $a = 0.3$ for organic liquids and $a = 0.15$ for water and low boiling liquids.

Values of the reference heat transfer coefficient α_0, the reference heat flux $\dot{q}_0$ and the surface roughness R_{po} are given in ref. [19].

The saturation temperature T_{Ph} at the interface is a function of the interface composition of liquid and vapour, which depend on the diffusion of each component in each phase. Gropp and Schlünder assume in ref. [18] that the mass transfer resistance in the vapour phase can be neglected because the velocity of the generated vapour streaming into the bubble is far higher than the velocity reached by a molecule due to diffusion in the vapour phase. The interface composition is, therefore, only controlled by the diffusion process on the liquid-side, where the velocity of the liquid moving towards the bubble interface has the same magnitude as the molecular velocity caused by diffusion. The evaporation of polynary mixtures results in a multicomponent, non-equimolar diffusion process. Lightfoot *et al.* showed in ref. [20], that the Stefan–Maxwell equations which were developed to describe multicomponent diffusion in dilute gases, can be applied to diffusion in liquids. Schlünder [21] suggests for this case to use the binary diffusion coefficients in the Stefan–Maxwell equations, resulting in the following form.

For ternary mixtures, equation (27) can then be transformed to give a set of three equations:

$$\rho_l \frac{\partial x_i}{\partial s} = \sum_{i=1}^{i=n} \frac{1}{\delta_{ji}}(x_j\cdot\dot{n}_i - x_i\cdot\dot{n}_j) \tag{28}$$

$$\frac{-\delta_{12}\rho_l}{\dot{n}}\cdot\frac{dx_1}{ds} = \dot{r}_1 - x_1 + \left(1-\frac{\delta_{12}}{\delta_{13}}\right)(x_1\dot{r}_3 - x_3\dot{r}_1) \tag{29a}$$

$$\frac{-\delta_{23}\rho_l}{\dot{n}}\cdot\frac{dx_2}{ds} = \dot{r}_2 - x_2 + \left(1-\frac{\delta_{23}}{\delta_{21}}\right)(x_2\dot{r}_1 - x_1\dot{r}_2) \tag{29b}$$

$$\frac{-\delta_{32}\rho_l}{\dot{n}}\cdot\frac{dx_3}{ds} = \dot{r}_3 - x_3 + \left(1-\frac{\delta_{32}}{\delta_{31}}\right)(x_3\dot{r}_1 - x_1\dot{r}_3) \tag{29c}$$

with

$$\dot{r}_j = \frac{\dot{n}_j}{\dot{n}} \quad \text{and} \quad \dot{n} = \sum_{i=1}^{3}\dot{n}_i.$$

Schlünder assumes that all binary diffusion coefficients have a similar value δ_l [21]. The bracketed terms in equations (29) will, therefore, disappear. This assumption allows us to extend this calculation procedure for polynary mixtures without the disadvantage of highly increased calculation times. Equations (29) can now be solved analytically and result in:

$$\frac{\dot{r}_i - x_i}{\dot{r}_i - x_{i,Ph}} = \exp\left(\frac{-\dot{n}s}{\rho_l\delta_l}\right). \tag{30}$$

Application of the film model [22] introduces the mass

transfer coefficient β_l as the ratio between the diffusion coefficient δ_l and the thickness s of the concentration boundary layer. The total molar flux $\dot{n}$ can be expressed as the ratio between the boiling heat flux $\dot{q}_{boil}$ and the heat of evaporation Δh_v. Since the mass transfer resistance on the vapour side is assumed to be zero one can conclude that the molar flux of a component $\dot{r}_i$ is equivalent to the vapour concentration of this component at the interface $y_{i,Ph}$. Equation (30) can therefore be written as:

$$\frac{y_{i,Ph}-x_i}{y_{i,Ph}-x_{i,Ph}}=\exp\left(\frac{-\dot{q}_{boil}\cdot 10^{-3}}{\rho_l\beta_l\Delta h_v M}\right). \tag{31}$$

This gives the relationship between the interface composition, the boiling heat flux and the mass transfer coefficient. Equation (31) can be solved by iteration to give the liquid concentration of each component at the interface. The vapour–liquid equilibria required for this calculation can be estimated using the Antoine equations for the vapour pressures and the Wilson equations for the activity coefficients. The saturation temperature corresponding to the liquid composition at the interface is the temperature T_{Ph} required in equation (22).

Instead of assuming constant binary diffusion coefficients, it is possible to estimate the binary diffusion coefficients of acetone, isopropanol and water using the Wilke–Chang method [23] in conjunction with the Vignes correlation [24], which takes into account the concentration dependency of the diffusion coefficients. The resulting values show that the binary diffusion coefficients of these components differ from each other and vary quite considerably with concentration, as can be seen in Fig. 3 for a temperature of 25°C. It should, therefore, be investigated if the accuracy of the calculation procedure outlined in the previous section can be improved by using individual, concentration dependent diffusion coefficients in equations (29). To do this, these equations have to be solved numerically using, for instance, a fourth order Runge–Kutta method. To estimate the thickness of the concentration boundary layer s in equations (28) it is assumed that mass transfer in the concentration boundary layer of a bubble is similar to unsteady heat transfer into a sphere. The same assumption has been made by Gropp and Schlünder [18] to estimate the liquid mass transfer coefficient. Since the concentration boundary layer can only exist during the lifetime of the bubble, the bubble frequency is calculated using a correlation by Malenkov [25], which includes the effect of the heat flux. Even though this correlation was found to be reliable by Malenkov, its application for subcooled conditions is doubtful. First tests by the authors showed a discrepancy of up to 30% between predicted and measured bubble frequencies for high subcoolings of the liquid. However, since there are no published correlations which consider the influence of subcooling, no other option is available.

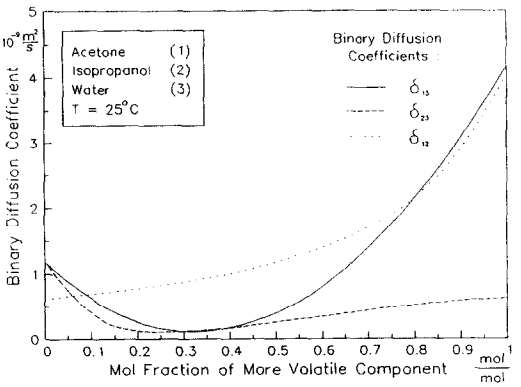

FIG. 3. Binary diffusion coefficients vs composition of binary mixture.

The authors found that the calculation with a concentration dependent diffusion coefficients led to wider discrepancies between the predictions of the programme and the measurements than the use of a constant diffusion coefficient δ_l. This is probably due to the difficulty of predicting the thickness of the concentration boundary layer, s. A further disadvantage of this solution method is the vastly increased calculation time. It is, therefore, recommended to use a constant diffusion coefficient δ_l and equation (30) in conjunction with the film model to find the composition of the liquid at the bubble interface and its saturation temperature T_{Ph}.

Output data

Output data are the heat transfer coefficient and the wall temperature.

COMPARISON BETWEEN PREDICTED AND MEASURED DATA

The mean error and the root mean square error

$$err_{ave}=\frac{1}{n}\sum_{i=1}^{n}\frac{|\alpha_{meas,i}-\alpha_{calc,i}|}{\alpha_{meas,i}} \tag{32}$$

$$err_{rms}=\left(\frac{1}{n}\sum_{i=1}^{n}\left(\frac{\alpha_{meas,i}-\alpha_{calc,i}}{\alpha_{meas,i}}\right)^2\right)^{0.5} \tag{33}$$

are used to assess the performance of the above prediction model. A comparison between predicted and measured heat transfer coefficients for the pure components showed a mean error of 8.58% and a root mean square error of 12.3%.

Two values for the mass transfer coefficient were used in equation (31) for comparison. The first value of 1×10^{-4} m s^{-1} is suggested by Gropp and Schlünder [18]. The comparison between the values calculated with this mass transfer coefficient and the experimental data show that the agreement can be improved by choosing a lower value. This is confirmed using a mass transfer coefficient of 0.5×10^{-4} m s^{-1}.

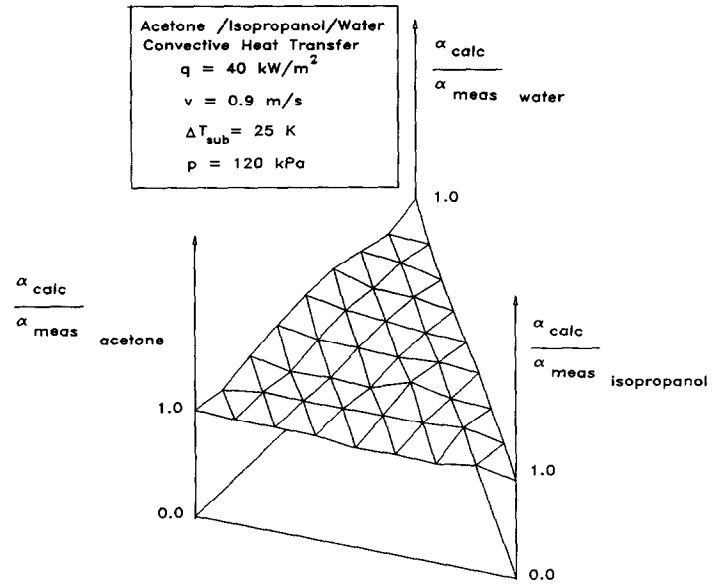

FIG. 4. Comparison of predicted and measured heat transfer coefficients for convective heat transfer.

The use of mass transfer coefficients smaller than 0.5×10^{-4} m s^{-1} did not result in a further significant improvement of the model's accuracy. The values for all the data available are given in Table 1.

The values for the mean and root mean square error are quite low, considering the wide range of subcooling, heat flux, fluid velocity and composition. The mass transfer coefficient is the only adjustable parameter of the model and these used for the calculation of the presented results are similar to values suggested in ref. [18]. In what follows, the performance of the model is investigated separately, for the forced convective and developed subcooled boiling regimes.

Convective heat transfer

Figure 4 illustrates the ratio between the predicted and measured values of the convective heat transfer coefficient. To show this ratio for all fluid compositions investigated a surface plot technique is used. The base area of this three dimensional illustration is the ternary mixture triangle. Each point on this triangle represents one investigated fluid mixture. According to the value given by the ratio of predicted to measured heat transfer coefficient, a specific height is assigned to each point on the ternary mixture triangle resulting in a three-dimensional surface. The heat transfer coefficients used for Fig. 4 were measured for a heat flux of 40 kW m^{-2}, a fluid velocity of 0.9 m s^{-1} and a subcooling of 25°C. The three-dimensional surface is rather smooth and appears to be almost parallel to the base triangle. This indicates that the difference between predicted and measured heat transfer coefficient is independent of the fluid composition. It is confirmed by the similar values for the mean error and the root mean square error of 6.32% and 7.11% for this set of data. Figure 5 shows the predicted and measured heat transfer coefficients for fluid mixtures with a constant water content of 12.5 mol%.

Table 1.

	$\beta_l = 0.5 \times 10^{-4}$ m s^{-1}	$\beta_l = 1.0 \times 10^{-4}$ m s^{-1}
Mean error	9.85%	11.06%
R.m.s. error	13.5%	15.62%

Nucleate boiling heat transfer

The ratio between the predicted and measured heat transfer coefficients under fully developed nucleate boiling conditions is illustrated in Fig. 6. The three-dimensional surface shown in this figure is rougher than the surface presented in Fig. 4. The highest peaks occur for binary mixtures of acetone/water and iso-

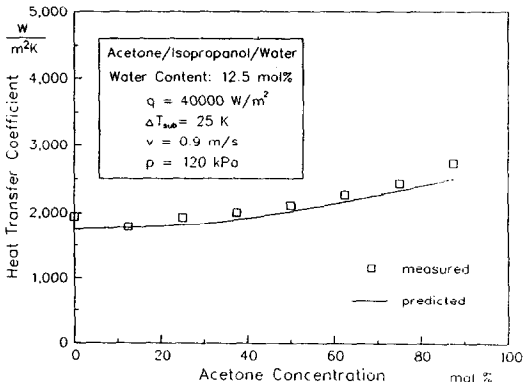

FIG. 5. Predicted and measured heat transfer coefficients over fluid compositions.

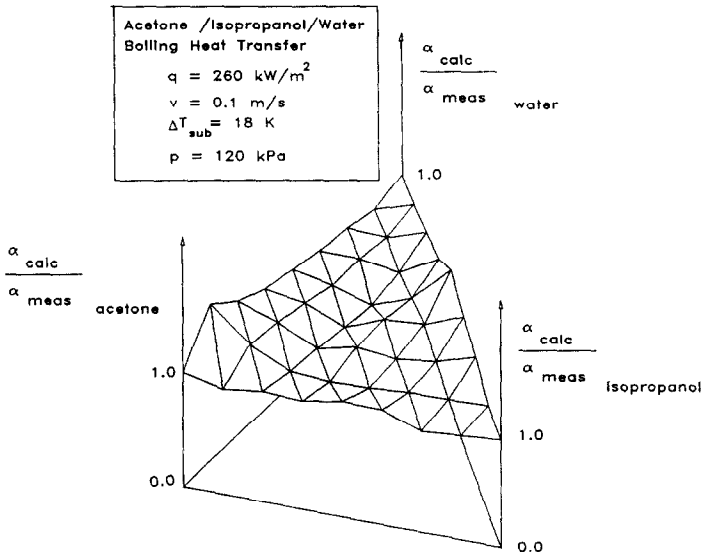

FIG. 6. Comparison of predicted and measured heat transfer coefficients for convective heat transfer.

propanol/water, indicating the highest differences between the measured and predicted values of the heat transfer coefficient. Figure 7 illustrates this, showing prediction and measurement for these binary systems. The largest discrepancies are found for 75.0 and 87.5 mol% of acetone in the acetone/water system and for 50.0 and 62.5 mol% of isopropanol in the isopropanol/water system. The measurements for the above mixtures do not agree well with data presented by Bajorek in ref. [26] and Wenzel in ref. [27], indicating that the large discrepancy in these two cases is most likely by dubious measurements and not by an inadequate prediction method. A complete data bank containing all experimental results and the predictions of this model can be found in ref. [28].

The mean error and the root mean square error for the set of data used in Fig. 6 have values of 7.59 and 11.33%, respectively. This mean error is considerably smaller than the values given in a recent publication by Bajorek *et al.* [29] for the same ternary system and several other prediction methods.

Full range of heat flux

Figure 8 shows measured and predicted heat transfer coefficients of an acetone/water mixture as a function of the heat flux. The predicted heat transfer coefficients compare favourably with the experimental data covering convective, transition and nucleate boiling heat transfer regimes. A comparison between 2400 measured and predicted heat transfer coefficients, covering the entire range of all system parameters, is presented in Fig. 9. The fairly uniform distribution of the points shown in this graph indicates that the model predicts the heat transfer coefficients reasonably well, independent of mechanism and magnitude of heat transfer.

Further development of this model should include the prediction of heat transfer at and just below

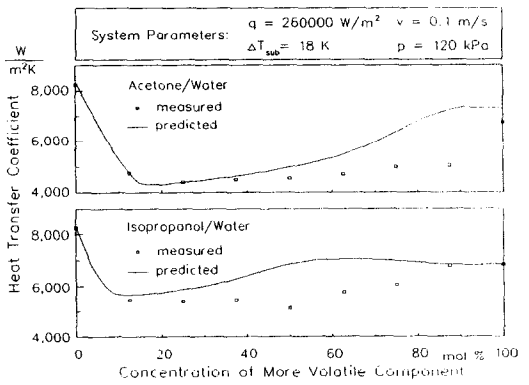

FIG. 7. Predicted and measured heat transfer coefficients over fluid compositions.

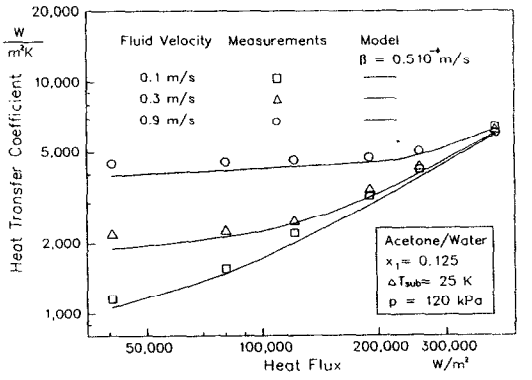

FIG. 8. Predicted and measured heat transfer coefficients vs heat flux.

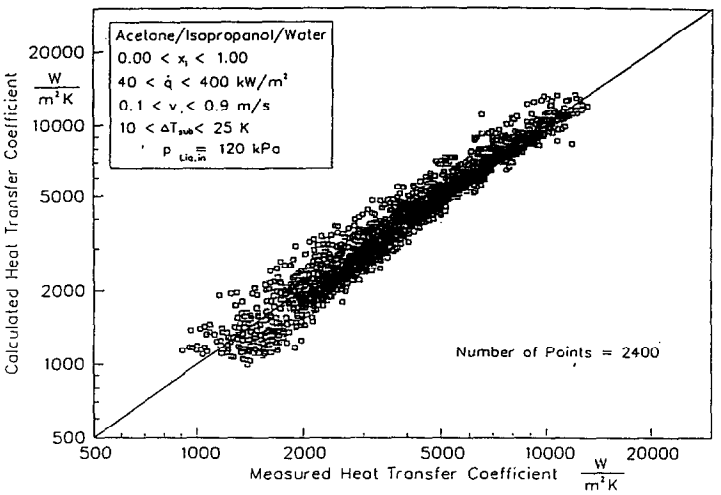

FIG. 9. Predicted vs measured heat transfer coefficients.

the critical heat flux. Unfortunately, no correlations have been published so far which reliably describe heat transfer for subcooled mixtures under such conditions.

Process liquors

The prediction model for subcooled flow boiling heat transfer outlined in this paper has also been tested against numerous data for Kraft Black liquor from the pulp and paper industry [30] and Bayer liquor from the alumina industry [31]. Both liquids are complex solutions with a high concentration of organic and inorganic materials. The solutions were considered as single component fluids ($\alpha_{boil} = \alpha_{id} = \alpha$) and the reference heat transfer coefficient α_o in equation (24) calculated using the Stefan and Preußer [32] correlation. For the full range of experimental conditions, the mean error for both fluids was less than 8%.

CONCLUSIONS

A model to predict local heat transfer coefficients for single component fluids, binary and ternary mixtures is presented. It is applicable for subcooled and saturated conditions, covering the regimes of convective, transition and fully developed nucleate boiling heat transfer. The model uses correlations for convective and pool boiling heat transfer, which are superimposed if the local wall temperature is higher than the saturation temperature of the fluid. It is expandable to mixtures with a larger number of components without difficulties.

A comparison between 2400 experimental data presented in Part I of this paper and the predictions of the model shows good agreement for all heat transfer regimes, independent of heat flux, subcooling, fluid composition and flow velocity.

REFERENCES

1. K. Stephan, *Wärmeübergang beim Kondensieren und beim Sieden*. Springer, Berlin (1988).
2. K. Spindler, N. Shen and E. Hahne, Vergleich von Korrelationen zum Wärmeübergang beim unterkühlten Sieden, *Wärme- und Stoffübertragung* **25**, 101–109 (1990).
3. J. C. Chen, Correlation for boiling heat transfer to saturated fluids in convective flow, *Ind. Engng Chem. Process Design and Development* **5**, 322–329 (1966).
4. J. G. Collier, Boiling within vertical tubes, *Heat Exchanger Design Handbook*, Sect. 2.7.3-12. McGraw-Hill, New York (1983).
5. J. J. Schröder, Wärmeübertragung beim unterkühlten Sieden, *VDI-Wärmeatlas*, Sect. Hba (4th Edn). VDI, Düsseldorf (1984).
6. S. Levy, Forced convection subcooled boiling—prediction of vapour volumetric fraction, *Int. J. Heat Mass Transfer* **10**, 951–965 (1967).
7. F. W. Dittus and L. M. K. Boelter, *Heat Transfer in Automobile Radiators of the Tubular Type*, Vol. 2, p. 13. University of California Press, California (1930).
8. V. Gnielinski, Wärmeübertragung bei der Strömung durch Rohre, *VDI-Wärmeatlas*, Sect. Gb (4th Edn). VDI, Düsseldorf (1984).
9. E. U. Schlünder, *Einführung in die Wärme- und Stoffübertragung*, p. 52. Vieweg, Braunschweig (1984).
10. R. K. Shah and A. L. London, Advances in heat transfer—Laminar flow forced convection in ducts, *Academic Press Supplement*, Vol. 1 (1978).
11. R. E. Lundberg, W. C. Reynolds and W. M. Kays, Heat transfer with laminar flow in concentric annuli with constant and variable wall temperature and heat flux, NASA Tech. Note TN D-1972 (1963).
12. R. E. Lundberg, P. A. McCuen and W. C. Reynolds, Heat transfer in annular passages. Hydrodynamically developed laminar flow with arbitrarily prescribed wall temperatures or heat fluxes, *Int. J. Heat Mass Transfer* **6**, 496–529 (1963).
13. B. S. Petukhov and V. N. Popov, Theoretical calculation of heat exchange and frictional resistance in turbulent flow in tubes of an incompressible fluid with variable physical properties, *High Temp. (USSR)* **1**, 69–83 (1963).
14. H. Hausen, Darstellung des Wärmeüberganges in Rohren durch verallgemeinerte Potenzbeziehungen, Z. Ver. Dtsch. Ing., *Beiheft Verfahrenstechnik* **4**, 91–134 (1943).

15. B. S. Petukhov and L. J. Roizen, Generalized relationship for heat transfer in turbulent flow of gas in tubes of annular section, *High Temp. (USSR)* **2,** 65–68 (1964).
16. G. K. Filonenko, Hydraulic resistance in pipes, *Teploenergetica* **1,** 40–44 (1954).
17. E. U. Schlünder, Einführung in die Lehre von der Wärmebertragung, *VDI-Wärmeatlas*, Sect. A (4th Edn). VDI, Düsseldorf (1984).
18. U. Gropp and E. U. Schlünder, The influence of liquid side mass transfer on heat transfer and selectivity during surface and nucleate boiling of liquid mixtures in a falling film, *Chem. Engng Process* **20,** 103–114 (1986).
19. D. Gorenflo, Behältersieden, *VDI-Wärmeatlas*, Sect. Ha (4th Edn). VDI, Düsseldorf (1984).
20. E. N. Lightfoot, E. L. Cussler and R. L. Rettig, Applicability of the Stefan Maxwell equations to multicomponent diffusion in liquids, *A.I.Ch.E. Jl* **8,** 708–710 (1962).
21. E. U. Schlünder, *Einführung in die Stoffübertragung*. Thieme, Stuttgart (1984).
22. R. B. Bird, W. E. Steward and E. M. Lightfoot, *Transport Phenomena*. Wiley, New York (1960).
23. C. R. Wilke and P. Chang, Correlation of diffusion coefficients in dilute solutions, *A.I.Ch.E. Jl* **1,** 264–270 (1955).
24. A. Vignes, Diffusion in binary solutions, *Ind. Engng Chem. Fundam.* **5,** 189–199 (1966).
25. I. G. Malenkov, The frequency of vapour-bubble separation as a function of bubble size, *Fluid Mech.—Sov. Res.* **1,** 36–42 (1972).
26. S. M. Bajorek, An experimental and theoretical investigation of multicomponent pool boiling on smooth and finned surfaces, Ph.D. Thesis, Department of Mechanical Engineering, Michigan State University (1988).
27. U. Wenzel, Unterkühltes Sieden bei der Strömung binärer Mischungen. Diploma Thesis Institut für thermische Verfahrenstechnik, Universität Karlsruhe, Karlsruhe, Germany (1989).
28. U. Wenzel, Saturated pool boiling and subcooled flow boiling of mixtures at atmospheric pressure, Ph.D. Thesis, University of Auckland, Auckland, New Zealand (1992).
29. S. M. Bajorek, J. R. Lloyd and J. R. Thome, Evaluation of multicomponent pool boiling heat transfer coefficients, *Proceedings of the 9th International Heat Transfer Conference*, Jerusalem, Israel, pp. 39–44 (1990).
30. M. Jamialahmadi and H. M. Müller-Steinhagen, Convective and subcooled boiling heat transfer to BAYER process liquor, *Light Metals* 141–150 (1992).
31. C. A. Branch and H. M. Müller-Steinhagen, Convective and subcooled boiling heat transfer to Kraft pulp black liquor, *APPITA J* (in press).
32. K. Stephan and P. Preußer, Wärmeübergang und maximale Wärmestromdichte beim Behältersieden binärer und ternärer Flüssigkeitsgemische, *Chem. Ing. Techn.* MS 649/79 (1979).